

EXPLORING THE DUST CONTENT OF GALACTIC WINDS WITH *HERSCHEL*.

II. NEARBY DWARF GALAXIES*

ALEXANDER McCORMICK,¹ SYLVAIN VAILLEUX,² MARCIO MELÉNDEZ,³ CRYSTAL L. MARTIN,⁴ JOSS BLAND-HAWTHORN,⁵
GERALD CECIL,⁶ FABIAN HEITSCH,⁶ THOMAS MÜLLER,⁷ DAVID S. N. RUPKE,⁸ AND CHAD ENGELBRACHT⁹

¹*Department of Physics, University of South Florida, Tampa, FL 33620, USA*

²*Department of Astronomy and Joint Space-Science Institute, University of Maryland, College Park, MD 20742*

³*NASA Goddard Space Flight Center, Greenbelt, MD 20771, USA ; Wyle Science, Technology and Engineering Group, 1290 Hercules Avenue, Houston, TX 77058, USA*

⁴*Department of Physics, University of California, Santa Barbara, CA 93106, USA*

⁵*Department of Physics, University of Sydney, Sydney, NSW 2006, Australia*

⁶*Department of Physics, University of North Carolina, Chapel Hill, NC 27599, USA*

⁷*Max-Planck-Institute for Extraterrestrial Physics (MPE), Giessenbachstrasse 1, 85748 Garching, Germany*

⁸*Department of Physics, Rhodes College, Memphis, TN 38112, USA*

⁹*Department of Astronomy, University of Arizona, Tucson, AZ 85721, USA (deceased)*

ABSTRACT

We present results from analysis of deep *Herschel Space Observatory* observations of six nearby dwarf galaxies known to host galactic-scale winds. The superior far-infrared sensitivity and angular resolution of *Herschel* have allowed detection of cold circumgalactic dust features beyond the stellar components of the host galaxies traced by *Spitzer* 4.5 μm images. Comparisons of these cold dust features with ancillary data reveal an imperfect spatial correlation with the ionized gas and warm dust wind components. We find that typically $\sim 10\text{-}20\%$ of the total dust mass in these galaxies resides outside of their stellar disks, but this fraction reaches $\sim 60\%$ in the case of NGC 1569. This galaxy also has the largest metallicity (O/H) deficit in our sample for its stellar mass. Overall, the small number of objects in our sample precludes drawing strong conclusions on the origin of the circumgalactic dust. We detect no statistically significant trends with star formation properties of the host galaxies, as might be expected if the dust were lifted above the disk by energy inputs from on-going star formation activity. Although a case for dust entrained in a galactic wind is seen in NGC 1569, in all cases, we cannot rule out the possibility that some of the circumgalactic dust might be associated instead with gas accreted or removed from the disk by recent galaxy interaction events, or that it is part of the outer gas-rich portion of the disk that lies below the sensitivity limit of the *Spitzer* 4.5 μm data.

Keywords: galaxies: dwarf — galaxies: halos — galaxies: interactions — galaxies: star formation —

- Данные последних лет: галактические ветра содержат пыль и молекулярный газ.
- Описывается: анализ “deep” данных HERSCHEL по 6 dlrr (70, 160, 250, 350, 500 мкм)+ H α and NIR
- We find circumgalactic dust features in all six galaxies of our sample. The most extended features range from 1.2 kpc (NGC 1800) to 2.6 kpc (He 2-10), as measured from the center of the galaxy or from the mid-plane of the disk-like region out to the furthest part of the feature.

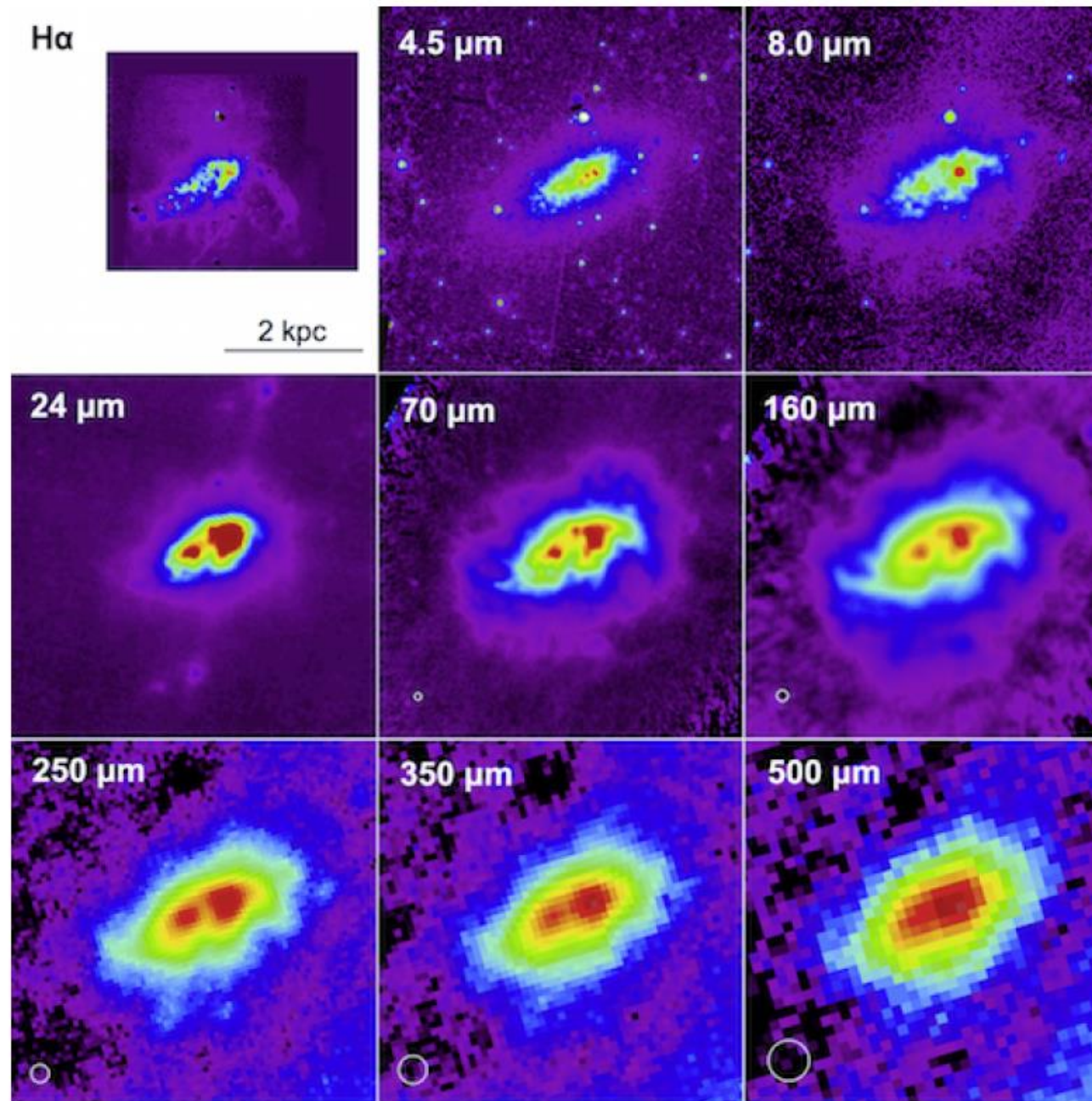
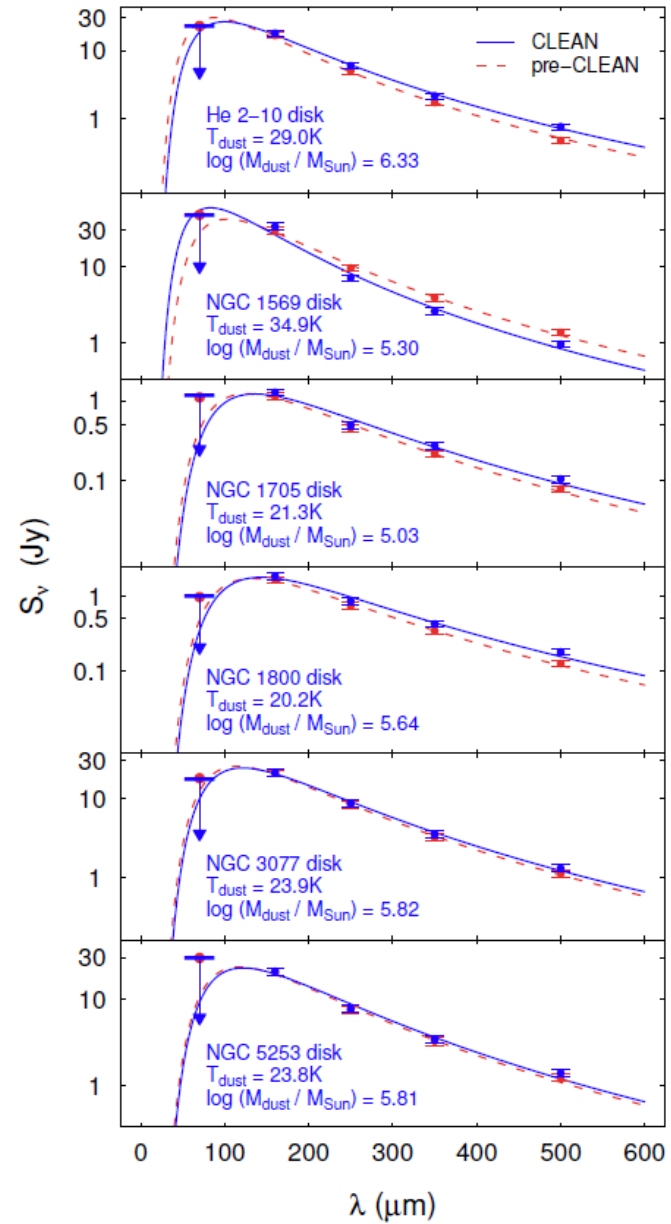


Figure 1b. NGC 1569 - $H\alpha$ (Martin 1997), IRAC 4.5 and 8.0 μm (McCormick et al. 2013), otherwise, the same as in Figure 1a.



ied blackbody fits to the galaxy disk fluxes derived from the 70, 160, 250, 350, and 500 μm (solid blue line) applying our modified CLEAN algorithm. In the fitting, the 70 μm flux by the downward arrows. The fit parameters are M_{dust} and T_{dust} . Refer to § 4.4 for det

Интегральные значения

- The fitted global cold dust masses are in the range 10^5 - $10^{6.5}$ M_{\odot} , implying gas-to-dust ratios of 200 - 1500.
- The circumgalactic features vary in morphology including extended filaments (NGC 1569, NGC 1705, NGC 1800, NGC 3077, and NGC 5253), clouds or knots of dust apparently separated from the disk region (NGC 1569, NGC 1705, and NGC 5253), as well as broader regions extending over a large range of galactocentric angles (e.g., He 2-10).

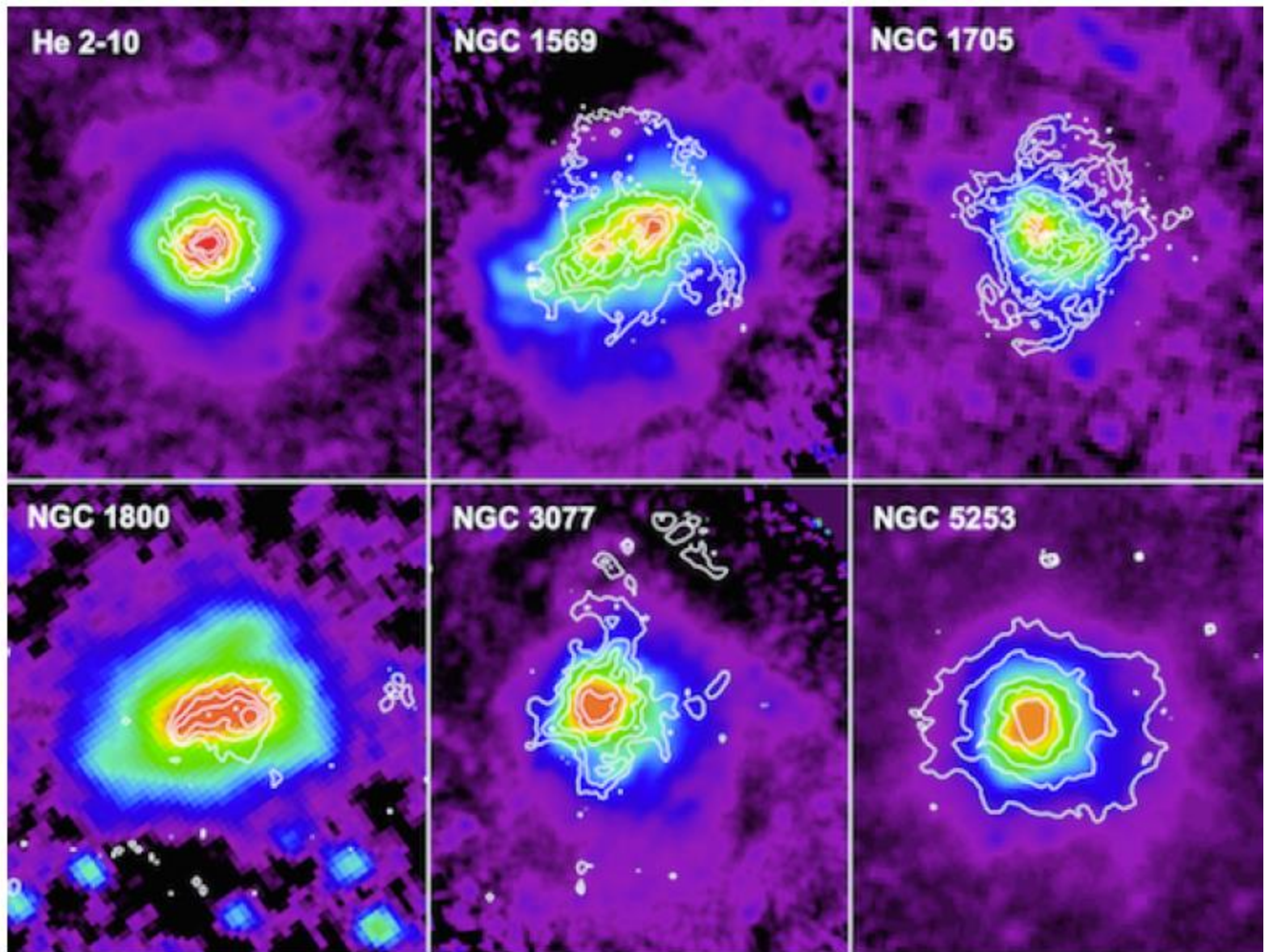


Figure 6. PACS $160\ \mu\text{m}$ maps overlaid with $\text{H}\alpha$ contours to compare the distribution of the cold dust with that of the warm ionized material. The field of view (FOV) of each panel is different to show the details at both $160\ \mu\text{m}$ and $\text{H}\alpha$. FOV: He 2-10 $3.96' \times 4.46'$; NGC 1569 $4.79' \times 5.40'$; NGC 1705 $3.13' \times 3.53'$; NGC 1800 $2.64' \times 2.98'$; NGC 3077 $5.23' \times 5.89'$; NGC 5253 $4.01' \times 4.52'$.

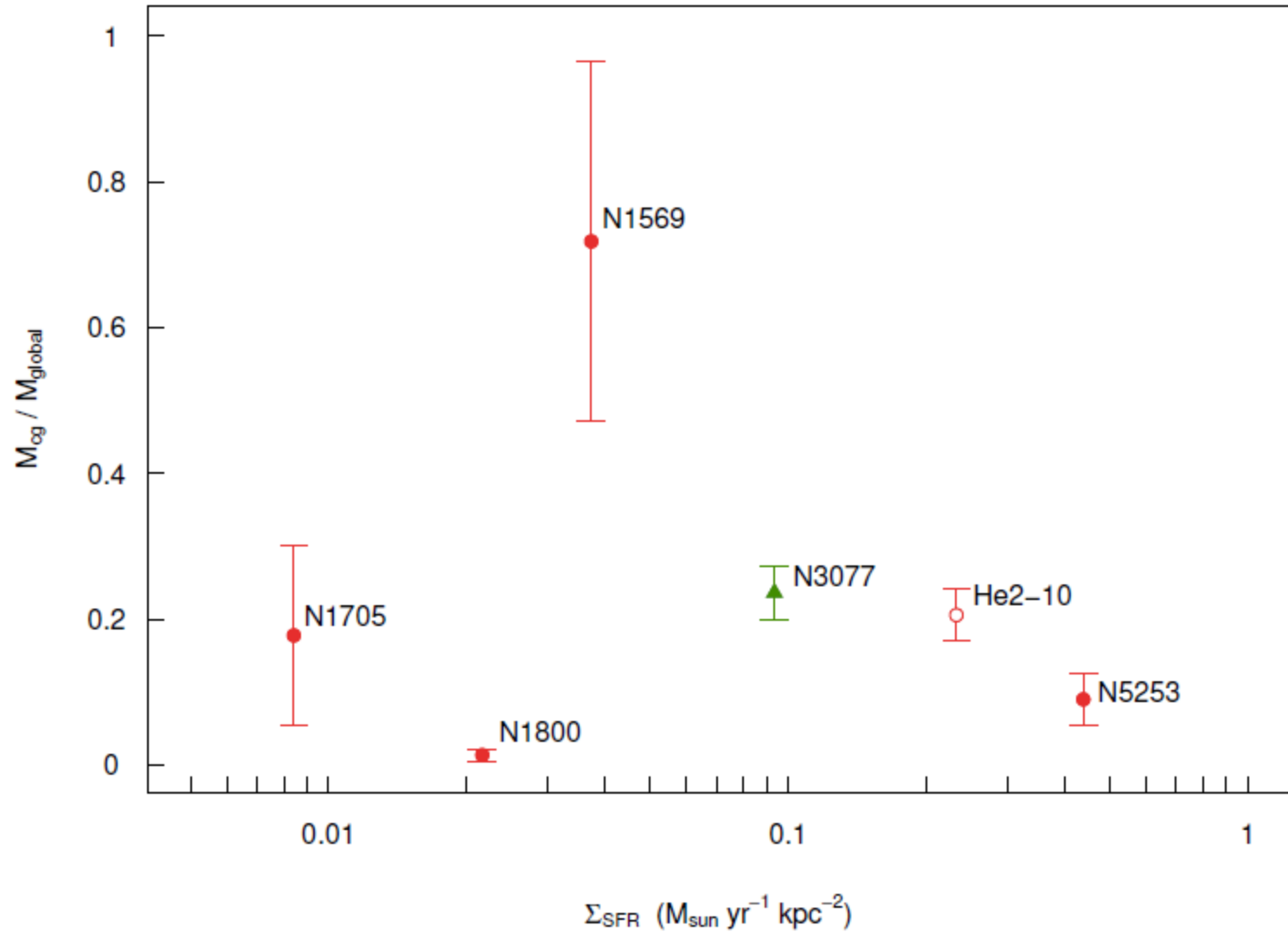


Figure 9. The circumgalactic dust mass fraction, M_{cg}/M_{global} , is plotted against the star formation rate surface density, Σ_{SFR} from Table 1. The uncertainty in M_{cg}/M_{global} comes from the uncertainties in the SED fitting (see § 4.4 and Table 5). The meaning of the symbols is the same as in Figure 8. No trend is seen in this figure between M_{cg}/M_{global} and Σ_{SFR} .

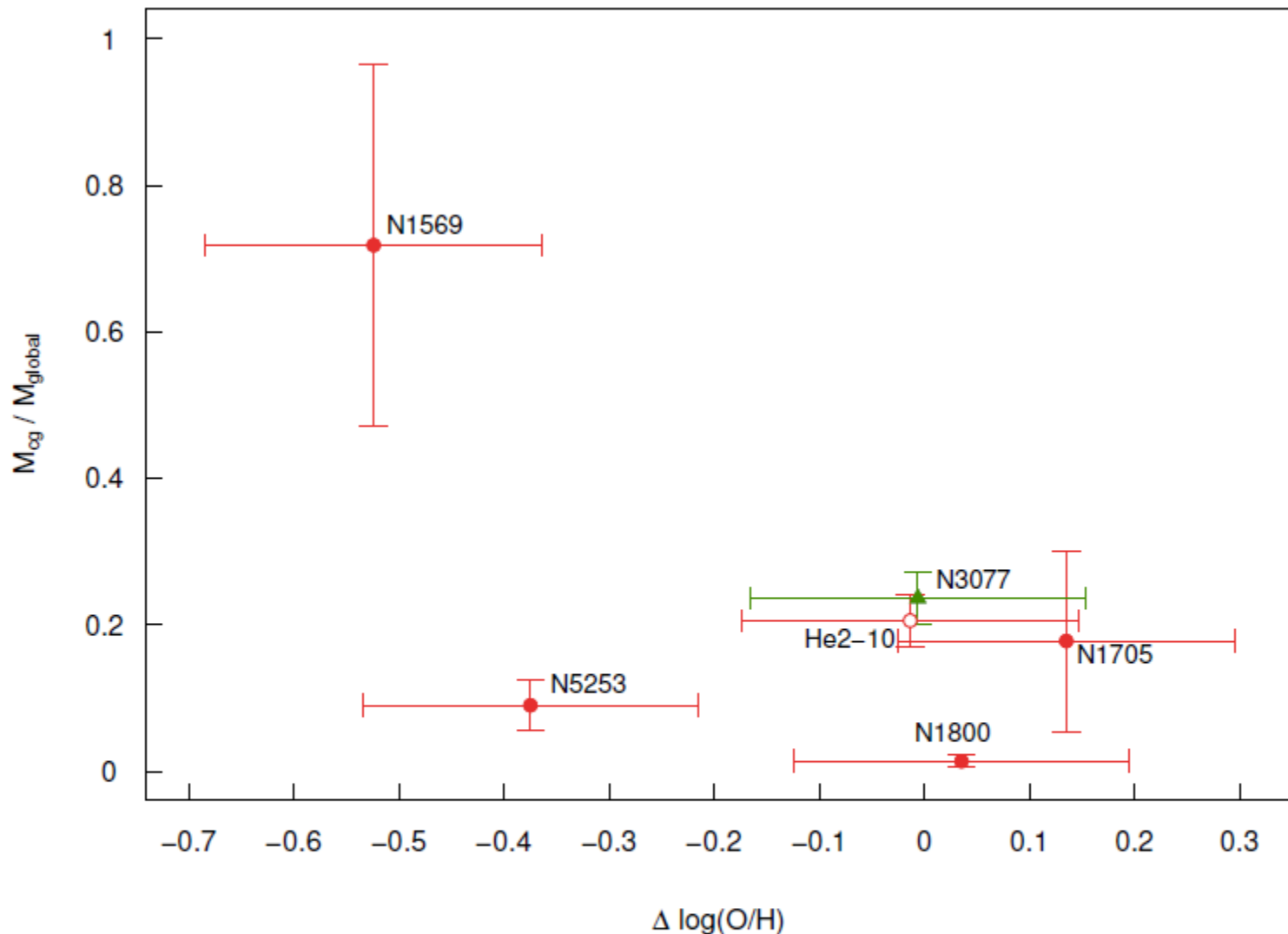


Figure 10. The circumgalactic dust mass fraction, M_{cg}/M_{global} , is plotted against the metallicity deficit, $\Delta \log(\text{O}/\text{H})$, defined as the difference between the galaxy metallicity (see Table 1) and the metallicity predicted by the relation derived in Tremonti et al. (2004) between M_* and $12 + \log(\text{O}/\text{H})$. The uncertainty on $\Delta \log(\text{O}/\text{H})$ comes from the uncertainty in the galaxy metallicity (~ 0.1 dex) and the uncertainty in converting values to conform with Tremonti et al. (2004) (~ 0.06 dex). The meaning of the symbols is the same as in Figure 8. No significant trend is seen in this figure between M_{cg}/M_{global} and $\Delta \log(\text{O}/\text{H})$, although the object (NGC 1569) with the largest circumgalactic dust mass fraction also has the largest metallicity deficit.

ОСНОВНЫЕ ВЫВОДЫ

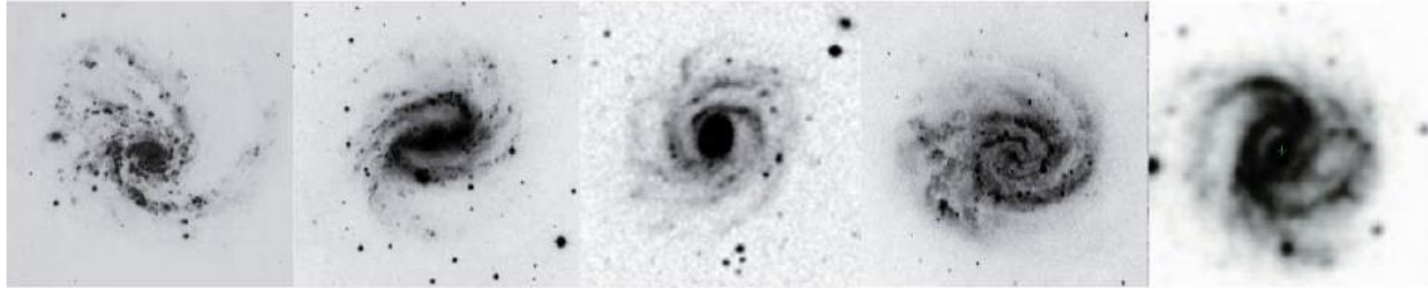
- We find that typically 10-20% of the total dust mass resides in the circumgalactic region, reaching a value as large as 60% in the case of NGC 1569.
- The presence of circumgalactic cold dust features in these dwarf galaxies does not obviously depend on the star formation rate surface density or gravitational influence of neighboring galaxies. The galaxy with the largest metallicity (O/H) deficit in our sample, NGC 1569, also happens to have the largest fraction of circumgalactic dust.
- Our data do not allow us to determine unambiguously the origin of the circumgalactic dust.

GALAXIES WITH “ROWS”: A NEW CATALOG

M. A. Butenko^{1,*} and A. V. Khoperskov^{1,**}

¹*Volgograd State University, Volgograd, 400062 Russia*

Galaxies with “rows” in Vorontsov-Velyaminov’s terminology stand out among the variety of spiral galactic patterns. A characteristic feature of such objects is the sequence of straight-line segments that forms the spiral arm. In 2001 A. Chernin and co-authors published a catalog of such galaxies which includes 204 objects from the Palomar Atlas. In this paper, we supplement the catalog with 276 objects based on an analysis of all the galaxies from the New General Catalogue and Index Catalogue. The total number of NGC and IC galaxies with rows is 406, including the objects of Chernin et al. (2001). The use of more recent galaxy images allowed us to detect more “rows” on average, compared with the catalog of Chernin et al. When comparing the principal galaxy properties we found no significant differences between galaxies with rows and all S-type NGC/IC galaxies. We discuss two mechanisms for the formation of polygonal structures based on numerical gas-dynamic and collisionless N-body calculations, which demonstrate that a spiral pattern with rows is a transient stage in the evolution of galaxies and a system with a powerful spiral structure can pass through this stage. The hypothesis of A. Chernin et al. (2001) that the occurrence frequency of interacting galaxies is twice higher among galaxies with rows is not confirmed for the combined set of 480 galaxies. The presence of a central stellar bar appears to be a favorable factor for the formation of a system of “rows”.



NGC 4254



NGC 4304



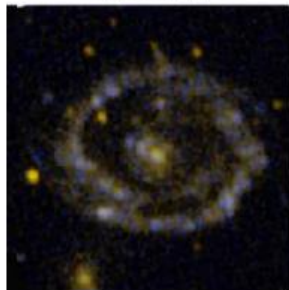
NGC 4897



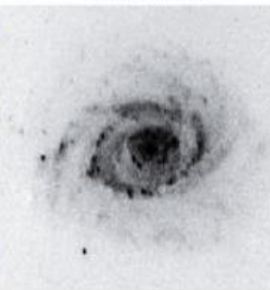
NGC 5861



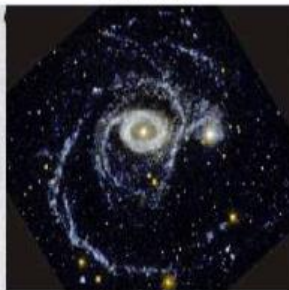
IC 2582



NGC 6962



NGC 5351



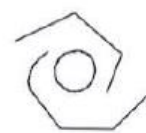
NGC 1512



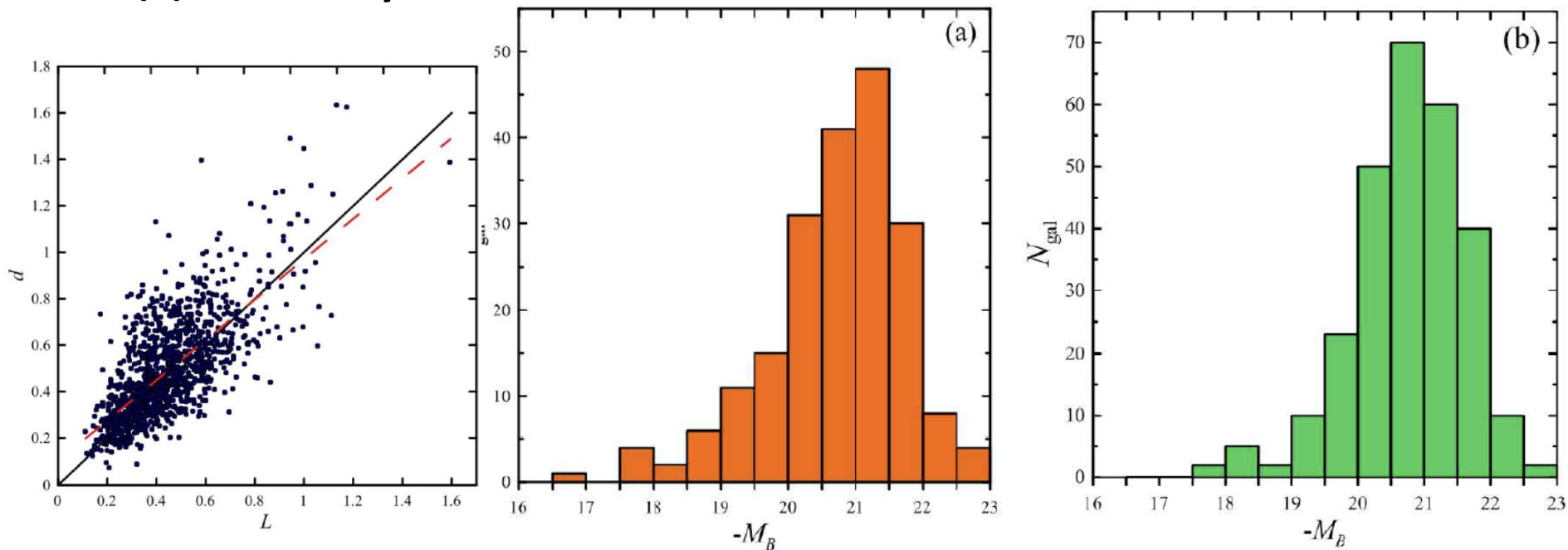
IC 577



IC 1562



- С использованием SDSS число объектов с вереницами более чем удвоилось, достигнув ~ 500 .



The "row length L – galactocentric distance d diagram (both quantities are normalized by the radius of the galaxy, $D_{25}/2$). The dashed and solid lines show the regression relation and the relation $d = L$, respectively

Figure 3. Distribution of absolute magnitudes of galaxies: (a) for all galaxies of the sample of Chernin et al. [3]; (b) for our sample of galaxies.

Два механизма фоормирования:

- Газодинамический:

Неустойчивость и спрямление фронта сильной ударной волны.

- Бесстолкновительный (предложен здесь):

Транзиентная стадия связанная с формированием бара. Возникают только в моделях с $\mu = M_h/M_d > 3$ within the optical radius и $Q_T < \sim 1$ – N-body models. These structures arise rather seldom and for a short time, usually during the initial stages of the development of gravitational instability.

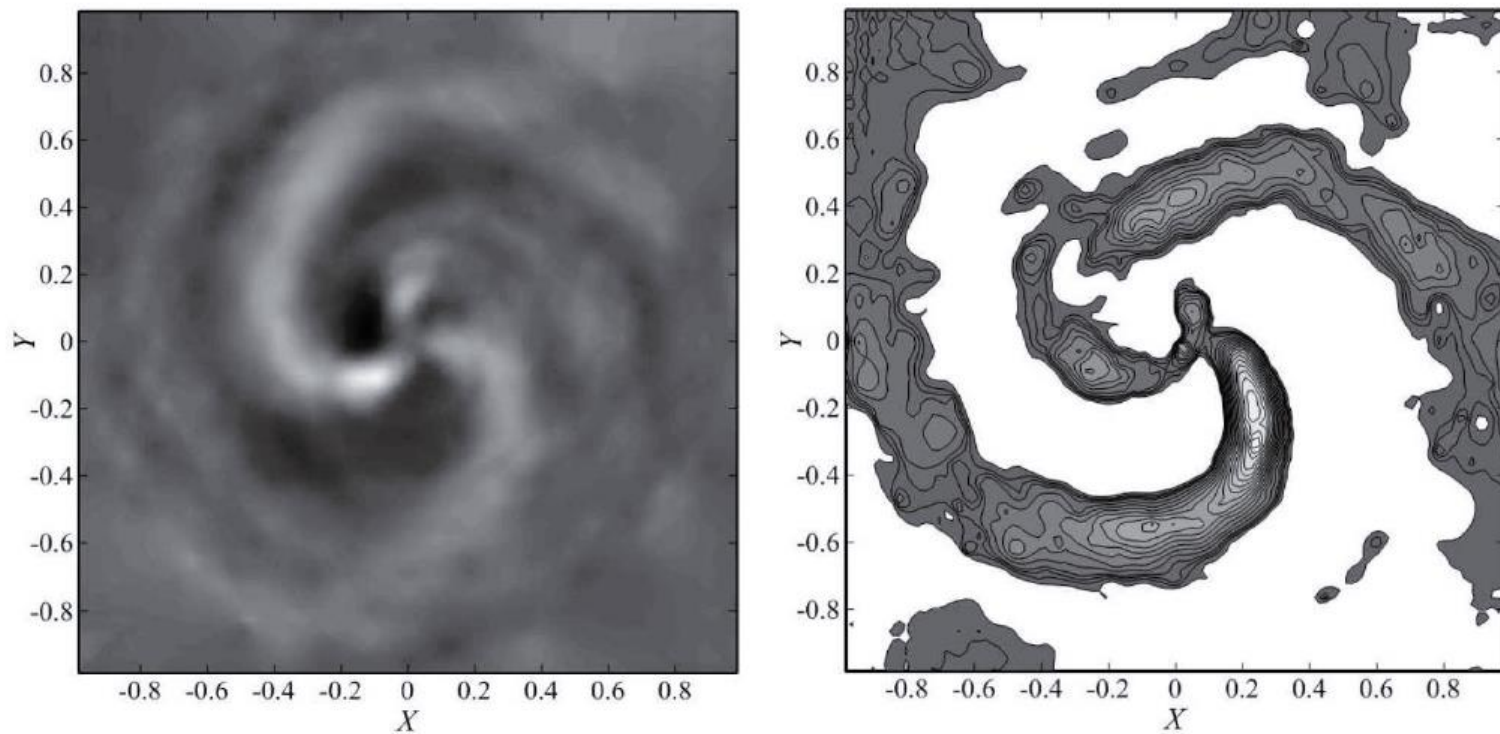


Figure 11. Distribution of the perturbation of surface density logarithm in the model stellar disk at different time instants (the left-hand panel shows only the positive part of the perturbation). At the initial time instant the Toomre parameter in the region $1/2 \lesssim r/r_d \lesssim 2$ is $Q_T = 0.8$, where r_d is the exponential disk scale.

- В старых звёздных дисках вереницы наблюдаются только в редких случаях (по 2MASS) (NGC4303, 5156, IC5325).
- Частота встречаемости по всем типам— 6%, из этих галактик 77% имеют бары, 38% - внутренние кольца, 27% - взаимодействующие. Флокуллентные ветви – в 12%, но в 40% спиральный узор не имеет чёткой структуры.
- Вереницы – транзиентные образования.

N4303 2MASS

1"
Powered by Aladin

5.553' x 3.616'

SDSS9 color-4

N4303_SDSS

1"
Powered by Aladin

9.596' x 6.249'



IC5325



A Virgo Environmental Survey Tracing Ionised Gas Emission (VESTIGE).III. Star formation in the stripped gas of NGC 4254[★],

A. Boselli^{1★★}, M. Fossati^{2,3}, J.C. Cuillandre⁴, S. Boissier¹, M. Boquien⁵, V. Buat¹, D. Burgarella¹, G. Consolandi^{6,7}, L. Cortese⁸, P. Côté⁹, S. Côté⁹, P. Durrell¹⁰, L. Ferrarese⁹, M. Fumagalli¹¹, G. Gavazzi⁶, S. Gwyn⁹, G. Hensler¹², B. Koribalski¹³, J. Roediger⁹, Y. Roehlly¹⁴, D. Russeil¹, M. Sun¹⁵, E. Toloba¹⁶, B. Vollmer¹⁷, A. Zavagno¹

ABSTRACT

During pilot observations of the Virgo Environmental Survey Tracing Galaxy Evolution (VESTIGE), a blind narrow-band H α + [NII] imaging survey of the Virgo cluster carried out with MegaCam at the CFHT, we have observed the spiral galaxy NGC 4254 (M99). Deep H α + [NII] narrow-band and GALEX UV images revealed the presence of 60 compact (70-500 pc radius) star forming regions up to ≈ 20 kpc outside the optical disc of the galaxy. These regions are located along a tail of HI gas stripped from the disc of the galaxy after a rapid gravitational encounter with another Virgo cluster member that simulations indicate occurred 280-750 Myr ago. We have combined the VESTIGE data with multifrequency data from the UV to the far-infrared to characterise the stellar populations of these regions and study the star formation process in an extreme environment such as the tails of stripped gas embedded in the hot intracluster medium. The colour, spectral energy distribution (SED), and linear size consistently indicate that these regions are coeval and have been formed after a single burst of star formation that occurred $\lesssim 100$ Myr ago. These regions might become free floating objects within the cluster potential well, and be the local analogues of compact sources produced after the interaction of gas-rich systems that occurred during the early formation of clusters.

1803.04177

- A surprising result of these recent studies is that only in a few cases does the stripped gas collapse to form stars outside the disc of the perturbed galaxy.
- This observational evidence is in contrast with the results of models and simulations which systematically predict the formation of new stars outside the galaxy disc (Kapferer et al. 2009; Tonnesen & Bryan 2010, 2012), an indication that the physical prescriptions used in the models need still to be refined.

VESTIGE (A Virgo Environmental Survey Tracing Ionised Gas Emission; Boselli et al. 2018, paper I) is a deep narrowband H imaging survey of the Virgo cluster carried out with MegaCam at the CFHT. This survey is providing us with a unique opportunity to study the fate of the stripped gas in cluster galaxies, being the first complete narrow-band imaging survey of a nearby cluster up to its virial radius (covering an area of $104^{\circ 2}$).

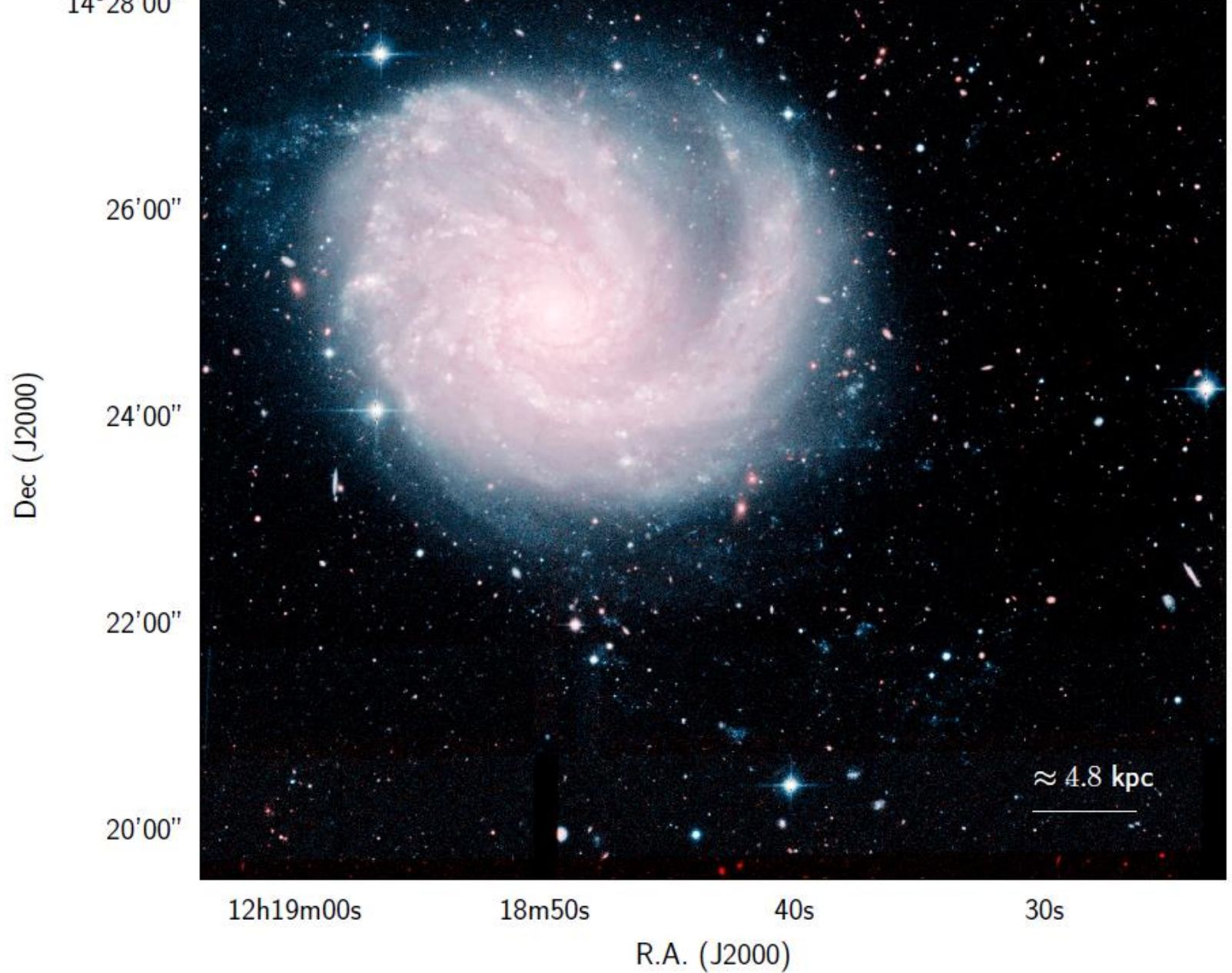


Fig. 1. Colour *ugi* RGB image of the galaxy NGC 4254 obtained using the NGVS data (Ferrarese et al. 2012). At the distance of the galaxy (16.5 Mpc), 1 arcmin = 4.8 kpc. The star forming regions analysed in this work are the blue blobs in the south-west outside the disc of the galaxy.

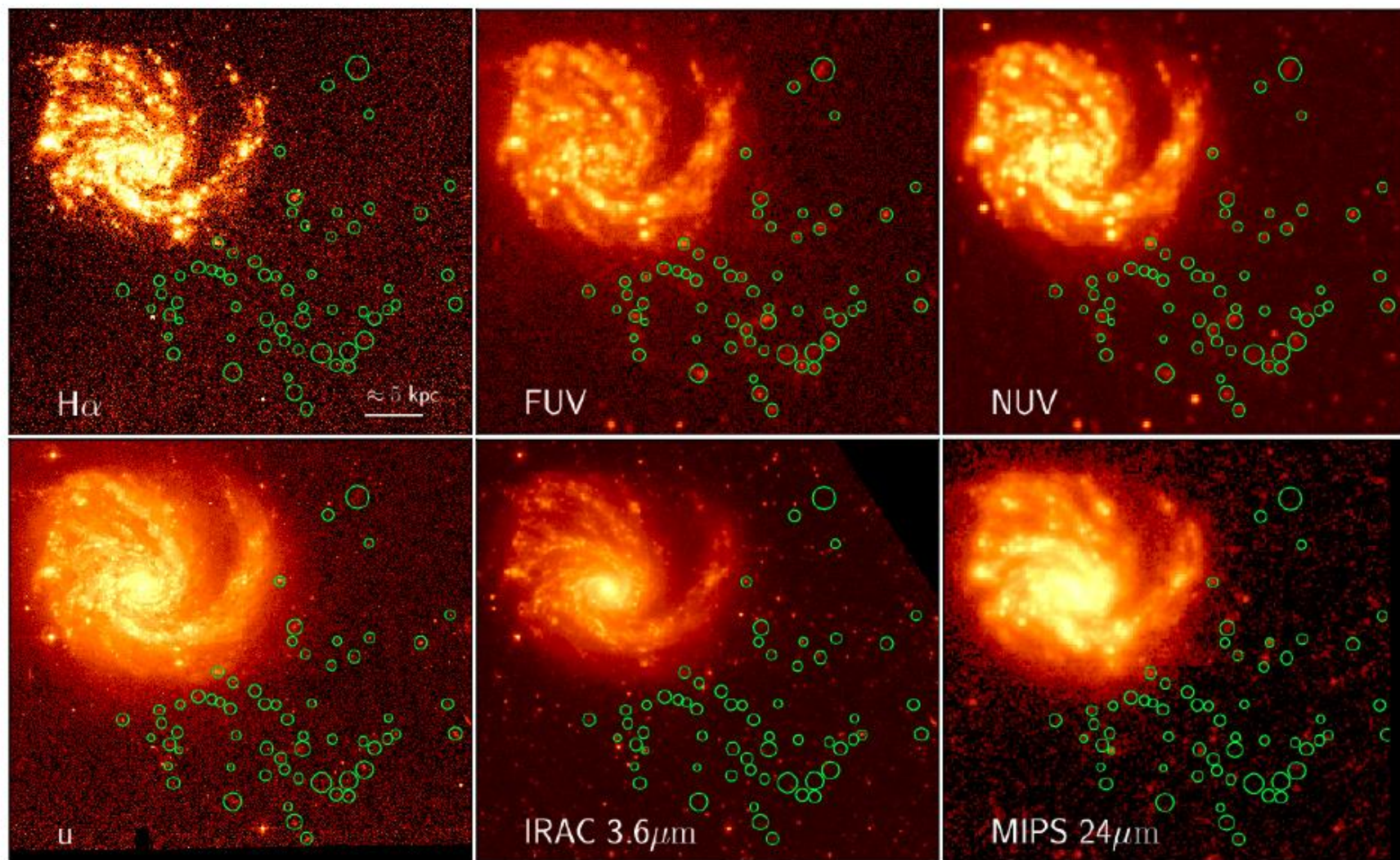


Fig. 2. Multifrequency images of the galaxy NGC 4254 (north is up, east is left). Upper panels, from left to right: continuum-subtracted H α (VESTIGE), *FUV* (GALEX), *NUV* (GALEX); lower panels: *u*-band (NGVS), IRAC 3.6 μm (*Spitzer*), MIPS 24 μm (*Spitzer*). The extraplanar star forming regions, marked with green circles, are evident in *FUV* image at the south-west of the galaxy. The linear size of each single image corresponds $40 \times 35 \text{ kpc}^2$ at the distance of the galaxy.

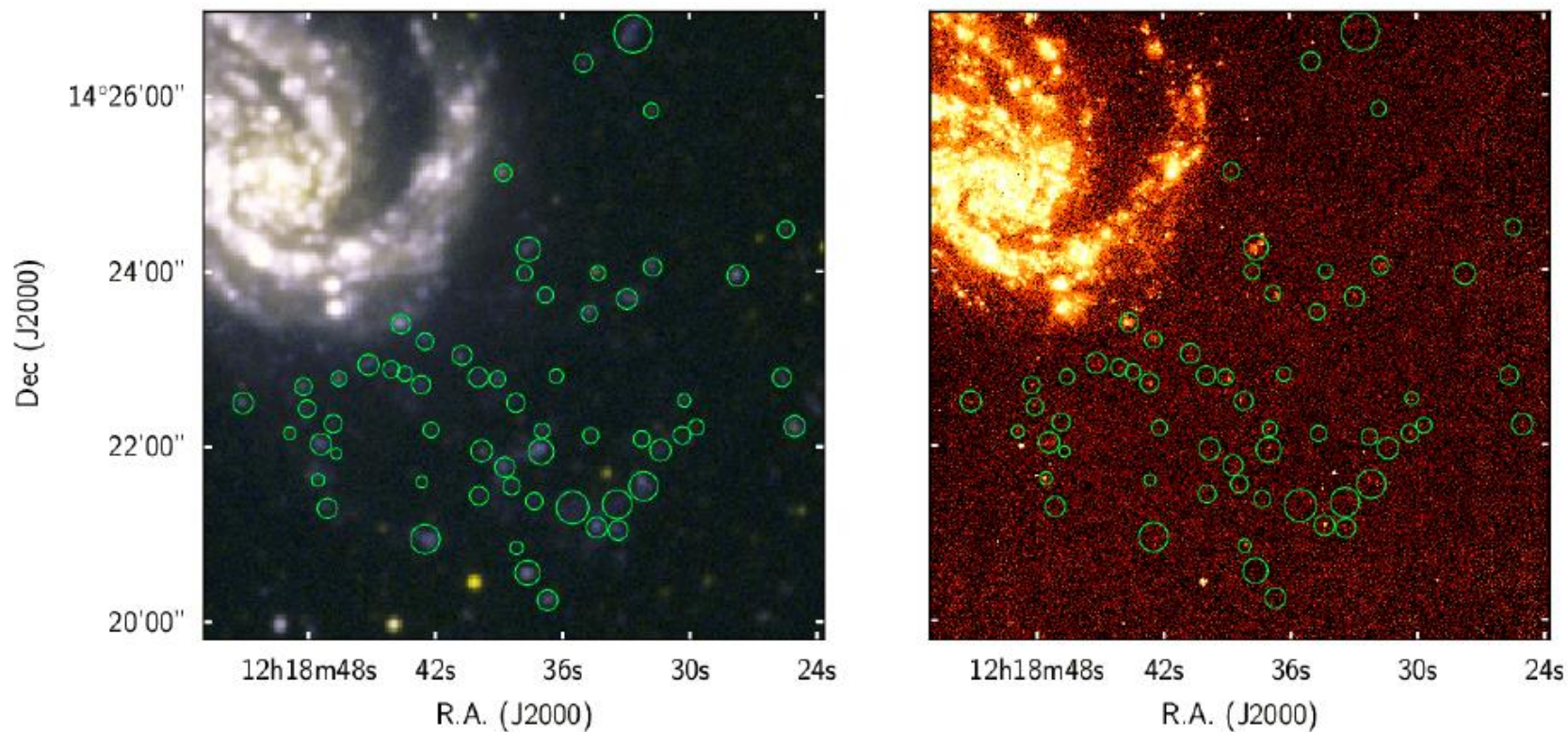


Fig. 3. FUV/NUV GALEX colour (left) and continuum-subtracted $H\alpha$ (VESTIGE; right) magnified images of the extraplanar star forming regions (marked with green circles) in the south-west quadrant of NGC 4254. The UV colour image shows that these regions have very blue colours, and are thus dominated by young stellar populations ($\lesssim 100$ Myr). Half of them, however, are undetected in $H\alpha$, indicating that their typical age is $10 \text{ Myr} \lesssim \text{age} \lesssim 100 \text{ Myr}$.

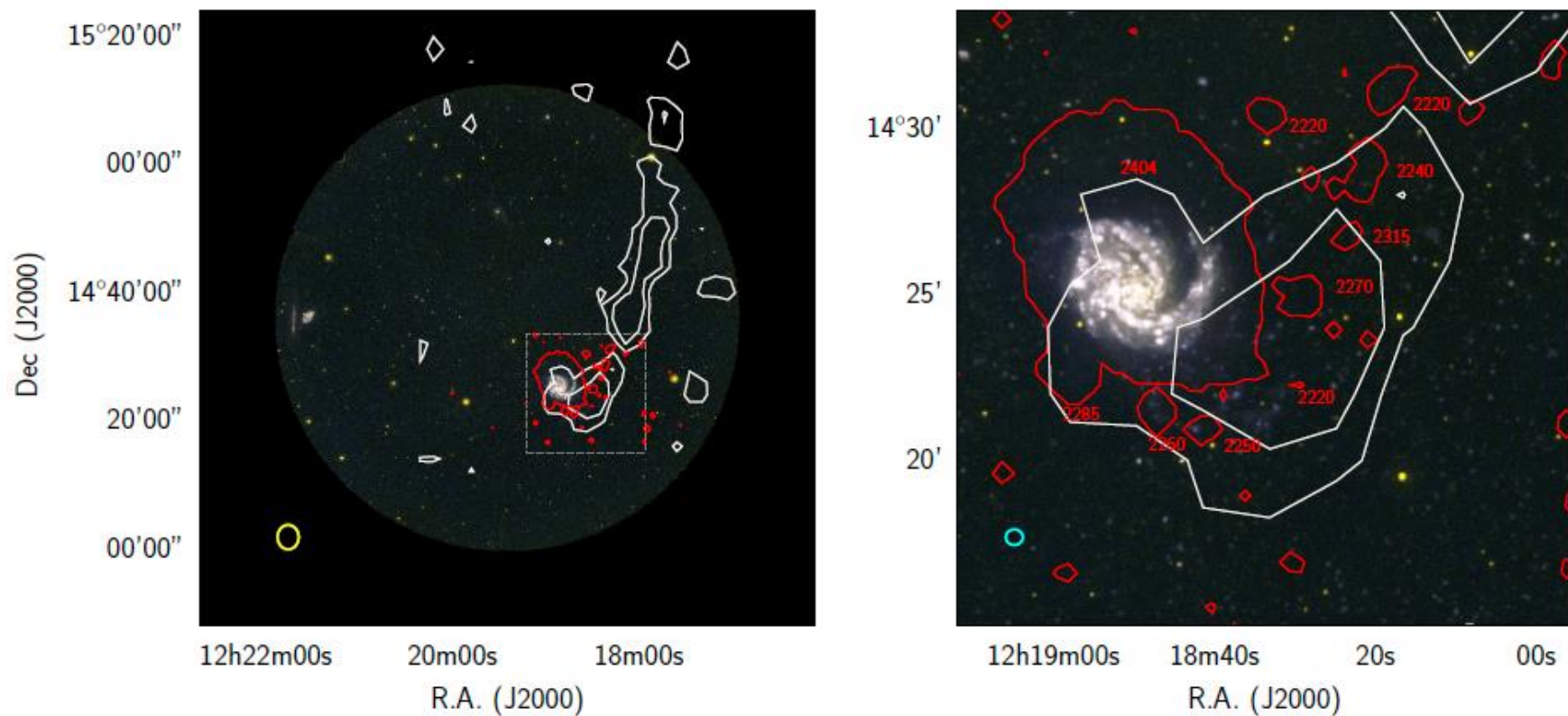


Fig. 4. The VLA HI contours at a column density $\Sigma(HI) = 10^{19} \text{ cm}^{-2}$ (from Chung et al. 2009; red) and the Arecibo HI contours at a column density $\Sigma(HI) = 1-2 \times 10^{19} \text{ cm}^{-2}$ (from Haynes et al. 2007; white) are superposed on the GALEX *FUV/NUV* colour image. The right panel is a magnified view of the boxed region marked in the left panel with a dashed line. The typical velocity of the different HI structures detected at the VLA are given. The yellow and cyan ellipses at the lower left corner of the two images show the beam sizes at Arecibo ($3.3' \times 3.8'$) and at the VLA ($30.86'' \times 28.07''$).

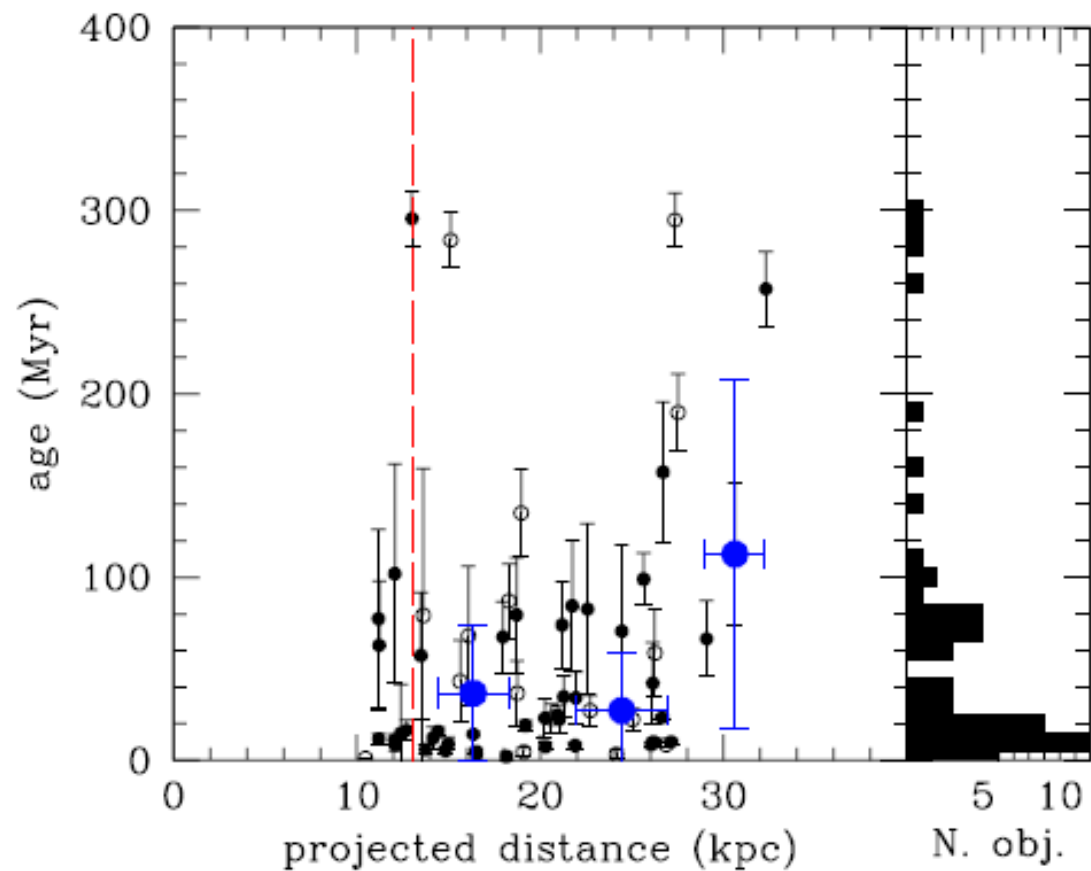


Fig. 12. Left panel: relationship between the age of the different H II regions as derived from CIGALE (in Myr) and their projected distance from the nucleus of NGC 4254 (in kpc). Filled dots indicates the H II regions where the SED fitting gives reduced $\chi_r^2 < 6$, empty dots $\chi_r^2 \geq 6$. Blue big filled dots indicate the median values within different distance bins. The red long-dashed vertical line indicates the 23.5 mag arcsec⁻² *i*-band isophotal radius of the galaxy given in Cortese et al. (2012b) Right panel: age distribution of all the H II regions.

Основной вывод:

- SED и линейный размер совместимы с одновременным образованием голубых эмиссионных областей менее 10^8 лет назад в результате gas stripping.
- По крайней мере некоторые из областей HII будут потеряны галактикой, превращаясь в межгалактические шаровые скопления, либо в stripped remnants типа AGC 226067 около M86, но не столь массивные, как в эпоху формирования скоплений.

